



OPEN

Spatial patterns and climate drivers of malaria in three border areas of Brazil, Venezuela and Guyana, 2016–2018

Kinley Wangdi^{1,7}✉, Erica Wetzler^{2,7}, Horace Cox³, Paola Marchesini⁴, Leopoldo Villegas^{5,6} & Sara Canavati²

In 2020, 77% of malaria cases in the Americas were concentrated in Venezuela, Brazil, and Colombia. These countries are characterized by a heterogeneous malaria landscape and malaria hotspots. Furthermore, the political unrest in Venezuela has led to significant cross-border population movement. Hence, the aim of this study was to describe spatial patterns and identify significant climatic drivers of malaria transmission along the Venezuela-Brazil-Guyana border, focusing on Bolivar state, Venezuela and Roraima state, Brazil. Malaria case data, stratified by species from 2016 to 2018, were obtained from the Brazilian Malaria Epidemiology Surveillance Information System, the Guyana Vector Borne Diseases Program, the Venezuelan Ministry of Health, and civil society organizations. Spatial autocorrelation in malaria incidence was explored using Getis-Ord (Gi*) statistics. A Poisson regression model was developed with a conditional autoregressive prior structure and posterior parameters were estimated using the Bayesian Markov chain Monte Carlo simulation with Gibbs sampling. There were 685,498 malaria cases during the study period. *Plasmodium vivax* was the predominant species (71.7%, 490,861). Malaria hotspots were located in eight municipalities along the Venezuela and Guyana international borders with Brazil. *Plasmodium falciparum* increased by 2.6% (95% credible interval [CrI] 2.1%, 2.8%) for one meter increase in altitude, decreased by 1.6% (95% CrI 1.5%, 2.3%) and 0.9% (95% CrI 0.7%, 2.4%) per 1 cm increase in 6-month lagged precipitation and each 1 °C increase of minimum temperature without lag. Each 1 °C increase of 1-month lagged maximum temperature increased *P. falciparum* by 0.6% (95% CrI 0.4%, 1.9%). *P. vivax* cases increased by 1.5% (95% CrI 1.3%, 1.6%) for one meter increase in altitude and decreased by 1.1% (95% CrI 1.0%, 1.2%) and 7.3% (95% CrI 6.7%, 9.7%) for each 1 cm increase of precipitation lagged at 6-months and 1 °C increase in minimum temperature lagged at 6-months. Each 1°C increase of two-month lagged maximum temperature increased *P. vivax* by 1.5% (95% CrI 0.6%, 7.1%). There was no significant residual spatial clustering after accounting for climatic covariates. Malaria hotspots were located along the Venezuela and Guyana international border with Roraima state, Brazil. In addition to population movement, climatic variables were important drivers of malaria transmission in these areas.

Abbreviations

AIC	Akaike's information criterion
CAR	Conditional autoregressive
CrI	Credible interval
DIC	Deviation information criterion

¹Department of Global Health, National Centre for Epidemiology and Population Health, ANU College of Health and Medicine, The Australian National University, Canberra, ACT 2601, Australia. ²World Vision US, 34834 Weyerhaeuser Way South, Federal Way, Washington, USA. ³Vector Borne Diseases Unit, Guyana Ministry of Health, Georgetown, Guyana. ⁴Department of Surveillance for Zoonotic and Vector Borne Diseases, Malaria Technical Group, Ministry of Health, Brasília, Federal District, Brazil. ⁵Global Development One, Silver Spring, MD, USA. ⁶Asociación Civil Impacto Social (ASOCIS), Tumeremo, Bolívar, Venezuela. ⁷These authors contributed equally: Kinley Wangdi and Erica Wetzler ✉email: kinley.wangdi@anu.edu.au

RR	Relative risk
SIVEP	MalariaBrazilian Malaria Epidemiology Surveillance Information System
SMRs	Standardized morbidity ratios
VIF	Variance inflation factors
WHO	World Health Organization

The WHO World Malaria Report 2021 showed that there were an estimated 241 million malaria cases and 627,000 malaria deaths worldwide in 2020. This represents about 14 million more cases in 2020 compared to 2019, and 69,000 more deaths. Approximately two-thirds of these additional deaths (47,000) were linked to disruptions in the provision of malaria prevention, diagnosis and treatment during the pandemic¹.

In the WHO Region of the Americas, malaria cases and case incidence reduced by 58% (from 1.5 million to 0.65 million) and 67% (from 14.1 to 4.6 cases per 1000 population at risk) between 2000 and 2020¹. Over the same period, there was reduction in both malaria deaths and the malaria mortality rate by 56% (from 909 to 409) and 66% (from 0.8 to 0.3 deaths per 100,000 population at risk), respectively¹. However, progress in this region suffered in recent years because of a major increase in malaria in the Bolivarian Republic of Venezuela, which had about 35,500 cases in 2000, rising to over 467,000 by 2019¹. In 2020, cases reduced to 232,000, or about half of 2019 cases¹. This was attributed to restrictions on movement during the COVID-19 pandemic and fuel shortages leading to reduced mining activities. As a result, occupational exposure risk to malaria vectors was significantly decreased¹.

So far, in the region, Argentina, Paraguay and El Salvador have eliminated malaria^{1–3}. Belize reported zero malaria cases for the second consecutive year in 2020¹. In addition, French Guiana, Guatemala, Honduras and Peru all met the global technical strategy 2020 malaria morbidity milestone of a reduction of at least 40% in case incidence¹. However, this progress has stalled in some places in recent years, with the rise in cases mainly due to the major increase in malaria in Venezuela^{2,4}. The country has been under a severe economic, political, and social crisis and all national institutions have been affected. The collapse of the Venezuelan health system has resulted in the deterioration of all facets of malaria prevention and control^{5,6}. Stock-outs of antimalarial drugs have been common, exacerbating malaria transmission⁵.

Furthermore, the political unrest in Venezuela has led to significant cross-border population movement⁷. More than 5.2 million people have left the country since 2015, and there has been a marked influx of Venezuelan nationals arriving in neighboring countries⁷. Malaria transmission in the WHO Region of the Americas is heterogeneous^{8,9} and four countries accounted for 77% of malaria cases in 20,202¹. Several factors are responsible for the continued transmission of malaria including climatic, ecological and human factors, further characterized by spatial clustering of cases in transmission hotspots^{10,11}. If malaria control interventions in hotspot areas are not sustained, these hotspots can serve as sources of infection to neighbouring regions and to countries that have eliminated malaria or where transmission has been interrupted^{12,13}. Delineation of malaria hotspots can help to identify the underlying reasons for higher incidence of malaria in particular areas¹⁴, which can serve to target interventions where they are most needed, likely having a greater impact than uniform resource allocation¹¹.

Spatial analysis and modelling enable the prediction of disease patterns and determination of ecological associations between disease risk and the environment^{11,15,16}. It is well known that geospatial methods can be used to link disease data to vector habitats, vector presence, abundance and density; quantify spatial diffusion; and characterize spatial and temporal patterns of disease^{17–24}. This paper aimed to describe spatial patterns and climatic drivers of malaria from 2016 to 2018 in Brazil (Roraima state), Venezuela (Bolívar state) and four regions of Guyana, all located in the Guyana Shield.

Methods

Study area and data. The study area included three border areas: Roraima state in Brazil, Bolívar state in Venezuela and four regions of Guyana (Fig. 1). Roraima and Bolívar are divided into 15 and 11 municipalities, respectively. Individual-level, de-identified datasets were obtained from national surveillance systems and additional sources: the Brazilian Malaria Epidemiology Surveillance Information System (SIVEP-Malaria), the Guyana Vector Borne Diseases Program, the Venezuelan Ministry of Health, and civil society organizations in Venezuela. Individual-level data were extracted on age, sex and malaria species. The populations of the municipalities were obtained from national census projections in each country^{25,26}. Monthly precipitation, and minimum and maximum temperature at 2.5 min intervals from January 2016 to December 2018 were obtained from the WorldClim database²⁷. Municipality polygon was used to extract the mean climatic variables using Zonal statistics in ArcMap 10.5.1 (ESRI Inc., Redlands, CA, USA). An electronic map of municipalities in shapefile format was obtained from the DIVA-GIS database (<https://www.diva-gis.org/>).

Hotspot analysis. The presence and nature of spatial autocorrelation that suggest malaria case clustering by place of notification were assessed by the Getis-Ord statistic (G_i^*)^{28,29}. The local Getis-Ord statistic (G_i^*) was used to identify the intensity and stability of hotspot/cold spot clusters^{29,30}. The G_i^* statistic compares the local malaria mean rate (i.e., the rate of malaria for a target location and its neighbors) to the global malaria mean rate (the rates of all municipalities). The G_i^* statistic compares the z-score and p-value for each municipality with global malaria means. Location with a statistically significant and larger z-score will have a more intense clustering of high values (hotspots), where it is unlikely that the spatial clustering of high values is the result of a random spatial process; and locations with statistically significant and smaller z-scores will have more intense clustering of low values (cold spots)²⁹. ArcMap 10.5.1 software (ESRI, Redlands, CA) was used for hotspot analysis and creating maps.



Figure 1. Map of the study areas.

Crude standardized morbidity ratios. An initial descriptive analysis of malaria incidence was conducted. Crude standardized morbidity ratios (SMRs) for each municipality were calculated using the following formula:

$$Y_i = \frac{O_i}{E_i}$$

where Y is the overall SMR in municipality i , O is the total number of observed malaria cases in the municipality and E is the expected number of malaria cases in the municipality across the study period. The expected

number was calculated by multiplying the national incidence by the average population for each municipality over the study period.

Independent variable selection. A preliminary Poisson regression was undertaken to select climatic covariates for each species. Climatic variables of precipitation, minimum and maximum temperature without a lag, and with one to 7-month lag times were entered into univariate models. Minimum temperature without lag, 1-month lagged maximum temperature and 6-month lagged precipitation had the lowest values of the Akaike's information criterion (AIC) for *P. falciparum* (Supplementary Table S1). Two-month maximum temperature and 6-month lagged precipitation and minimum temperature were selected for *P. vivax* with the lowest AIC (Supplementary Table S2). The co-linearity of the climatic variables was tested using variance inflation factors (VIF) (Supplementary Tables S3, S4).

Spatio-temporal model. Poisson regression models were developed in the Bayesian statistical software WinBUGS version 1.4 (Medical Research Council, Cambridge, UK and Imperial College London, UK) for *P. falciparum* and *P. vivax*. Alternative models were tested for each species including models with climatic variables such as precipitation, minimum and maximum temperature as explanatory variables, and spatially structured and unstructured random effects. The best model was selected based on the lowest deviation information criterion (DIC) for each species. Three models were developed: Model I consisted of climatic explorative variables and unstructured random effects; Model II contained the same explorative variables as Model I and spatially structured random effects. Model III contained both structured and unstructured random effects and climatic explorative variables. Model III was the most comprehensive model, which had as an outcome the observed counts of malaria, Y , for i^{th} municipality ($i = 1 \dots 30$) in the j^{th} month (January 2016–December 2018) was structured as follows:

$$Y_{ijkl} \sim \text{Poisson}(\mu_{ijkl})$$

$$\log(\mu_{ijkl}) = \log(E_{ijkl}) + \theta_{ijkl}$$

$$\theta_{ijkl} = \alpha + \beta_1 \times \text{trend} + \beta_2 \times \text{Altitude} + \beta_3 \times \text{Precipitation}_{ij} + \beta_4 \times \text{Tempmin}_{ij} + \beta_5 \times \text{Tempmax}_{ij} + u_i + s_j.$$

where E is the expected number of cases (acting as an offset to control for population size) and θ is the mean log relative risk (RR); α is the intercept, and $\beta_1, \beta_2, \beta_3, \beta_4$ and β_5 the coefficients for trend, altitude, precipitation, minimum and maximum temperature, respectively; u_i is the unstructured random effect (assumed to have a mean of zero and variance σ_u^2) and s_j is the spatially structured random effect (assumed to have a mean of zero and variance σ_s^2).

A conditional autoregressive (CAR) prior structure was used to model the spatially structured random effect. An adjacency weights matrix was used to calculate the spatial relationships between the municipalities. A weight of 1 was assigned if two municipalities shared a border and 0 if they did not. A flat prior distribution was specified for the intercept, whereas a normal prior distribution was specified for the coefficients. The priors for the precision of unstructured and spatially structured random effects were specified using non-informative gamma distributions with shape and scale parameters. Models were also developed without the structured and unstructured random effects to assess whether inclusion of these components improved model fit.

An initial burn-in of 10,000 iterations was run, and these iterations were discarded. Subsequent blocks of 20,000 iterations were run and examined for convergence. Convergence was assessed by visual inspection of posterior density and history plots, and occurred at approximately 100,000 iterations for each model. Ten thousand values from the posterior distributions of each model parameter were stored and summarized for the analysis (posterior mean and 95% credible intervals [CrI]).

In all analyses, an α -level of 0.05 was adopted to indicate statistical significance (as indicated by 95% CrI for RR that excluded 1). ArcMap 10.5.1 software (ESRI, Redlands, CA) was used to generate maps of the posterior means of the unstructured from the three models.

Ethics approval and consent to participate. The National Center of Bioethics in Venezuela (CENABI) approved the research protocol and the National Survey Ethics Council (CONEP) considered that ethical clearance for the use of this secondary data in Brazil was not necessary. Not applicable. Human participants were not involved in the study. This research uses secondary data and is not subject to ethics approval.

Results

Descriptive analysis. There were a total of 684,498 malaria cases recorded during the study period, and 88.3% (604,306) of these cases were reported from Bolivar state, Venezuela. Compared to 2016, malaria cases across the study areas increased from 25.5% (174,635) to 37.5% (256,482) and 37.0% (253,381) cases in 2017 and 2018, respectively. More than two-thirds of cases were in males (67.5%, 461,912). The predominant species was *P. vivax* (71.7%, 490,861) followed by *P. falciparum* (22.4%, 153,512). However, mixed infections with *P. vivax* and *P. falciparum* consisted of 4.6% (8,008), 5.7% (14,492) and 6.9% (17,381) in 2016, 2017 and 2018, respectively (Table 1). Mean precipitation, and minimum and maximum temperature were 150.5 mm (range 1.1–413.6 mm), 21.9 °C (range 16.9–24.6 °C) and 31.1 °C (range 26.8–35.2 °C), respectively (Supplementary Table S5). The *P. falciparum* SMR varied from 0.0 to 14.94 during the study period, and Pacaraima municipality in Roraima state and Sifontes municipality in Bolivar state reporting the highest SMR with ranges increasing each year: 2016

Characteristics	Year			p-value*
	2016	2017	2018	
Country	Number (%)	Number (%)	Number (%)	
Roraima, Brazil	8969 (5.1)	14,082 (5.5)	23,369 (9.2)	< 0.001
Guyana	8355 (4.8)	11,139 (4.3)	14,278 (5.6)	
Bolivar, Venezuela	157,311 (90.1)	23,1261 (90.2)	215,734 (85.1)	
Total	174,635 (25.5)	256, 482 (37.5)	253, 381 (37.0)	
Sex				
Female	53,839 (30.8)	83,136 (31.4)	85,611 (33.8)	< 0.001
Male	120,796 (69.2)	173,346 (76.6)	167,770 (66.2)	
Age category (years)				
0–18	41,123 (23.7)	62,715 (24.5)	61,618 (24.4)	< 0.001
19–30	63,891 (36.8)	89,782 (56.0)	89,926 (35.6)	
31–40	34,107 (19.6)	50,397 (19.7)	50,311 (19.9)	
40+	34,597 (19.9)	52,797 (20.7)	50,914 (20.1)s	
Species				
<i>P. falciparum</i>	37,217 (21.3)	53,138 (20.7)	63,157 (24.9)	< 0.001
<i>P. vivax</i>	129,354 (74.1)	188,755 (73.6)	172,752 (68.2)	
<i>P. malariae</i>	11 (0.0)	13 (0.0)	15 (0.0)	
Mixed	8008 (4.6)	14,492 (5.7)	17,381 (6.9)	

Table 1. Demographic characteristics of malaria from 2016 to 2018. *p-value significant at < 0.05.

(SMR 6.20–14.94), 2017 (SMR 4.45–14.28) and 2018 (SMR 6.1–17.04) (Fig. 2A). The *P. vivax* SMR varied from 0.0 to 18.78 during the study period with Sifontes municipality again reporting the highest SMR: 2016 (SMR 6.68–18.78), 2017 (SMR 8.42–17.14) and 2018 (SMR 6.07–18.18) (Fig. 2B).

Spatial autocorrelation. Applying the Getis-Ord G^* statistic hotspot analysis to *P. falciparum* and *P. vivax* incidence in each municipality revealed statistically significant ($p < 0.01$) hotspots in eight border municipalities of Venezuela and Guyana: Piar, Padre Pedro Chien, Roscio, El Callao and Sifontes in Bolivar state and Barina-Waini and Cuyuni-Mazaruni in Guyana (Figs. 3, 4).

Spatio-temporal model. Model I, containing the unstructured random effect, had the best fit and was the most parsimonious of all the models, examined for both *P. falciparum* and *P. vivax*, as indicated by the lowest DIC (Table 2). For *P. falciparum*, monthly malaria cases increased by 2.1% (95% CrI 2.0%, 2.1%) per month during the study period. One meter increase in altitude increased malaria cases by 2.6% (95% CrI 2.1%, 2.8%). While one cm increase in 6-month lagged precipitation and each 1 °C increase of minimum temperature were associated with 1.6% (95% CrI 1.5%, 2.3%) and 0.9% (95% CrI 0.7%, 2.4%) decrease of *P. falciparum*, respectively. Each 1 °C increase of 1-month lagged maximum temperature increased *P. falciparum* by 0.6% (95% CrI 0.4%, 1.9%). Monthly *P. vivax* increased by 1.0% (95% CrI 0.9%, 1.0%) during the study period. *P. vivax* cases increased by 1.5% (95% CrI 1.3%, 1.6%) for one meter increase in altitude and decreased by 1.1% (95% CrI 1.0%, 1.2%) for each cm increase of precipitation lagged at 6-months and 7.3% (95% CrI 6.7%, 9.7%) for each 1 °C increase in minimum temperature lagged at 6-months. Each 1 °C increase of two-month lagged maximum temperature increased *P. vivax* by 1.5% (95% CrI 0.6%, 7.1%) (Table 2). There is no evidence of spatial clustering after accounting for model covariates, - meaning covariates in the model explained the transmission of malaria and there was no effect from malaria transmission in the adjoining municipalities (Fig. 5).

Discussion

This study aimed to describe spatial patterns and climatic drivers of malaria in the border states of Brazil, Venezuela and Guyana using national malaria surveillance data from 2016 to 2018. The great majority of malaria cases were reported from Bolivar state in Venezuela: 157,311 (90.1%), 231,261 (90.2%), and 215,734 (85.1%) from 2016 to 2018, respectively. The most commonly reported malaria species was *P. vivax* (490,861, 71.7%). Hotspots of both *P. falciparum* and *P. vivax* were located in the border municipalities of Venezuela and Guyana. *P. falciparum* transmission was positively associated with altitude and maximum temperature lagged at 1-month, and negatively associated with precipitation lagged at 6-months and minimum temperature without lag. Whereas *P. vivax* was positively associated with altitude and maximum temperature lagged at 2-months and negatively associated with precipitation and minimum temperature lagged at 6-months.

Since 1990, the majority of malaria cases in Venezuela have come from Bolivar state: > 60% (1992–1995) and 88% (2000–2014)^{7,31–33}, with most cases clustering in Sifontes municipality (Bolivar State)⁷. Additionally, in Sifontes municipality, gold mining has been associated with a high incidence of malaria, with miners accounting for up to 80% of cases^{8,9,31,34}. In contrast to progress made in neighboring countries and in the Americas, the

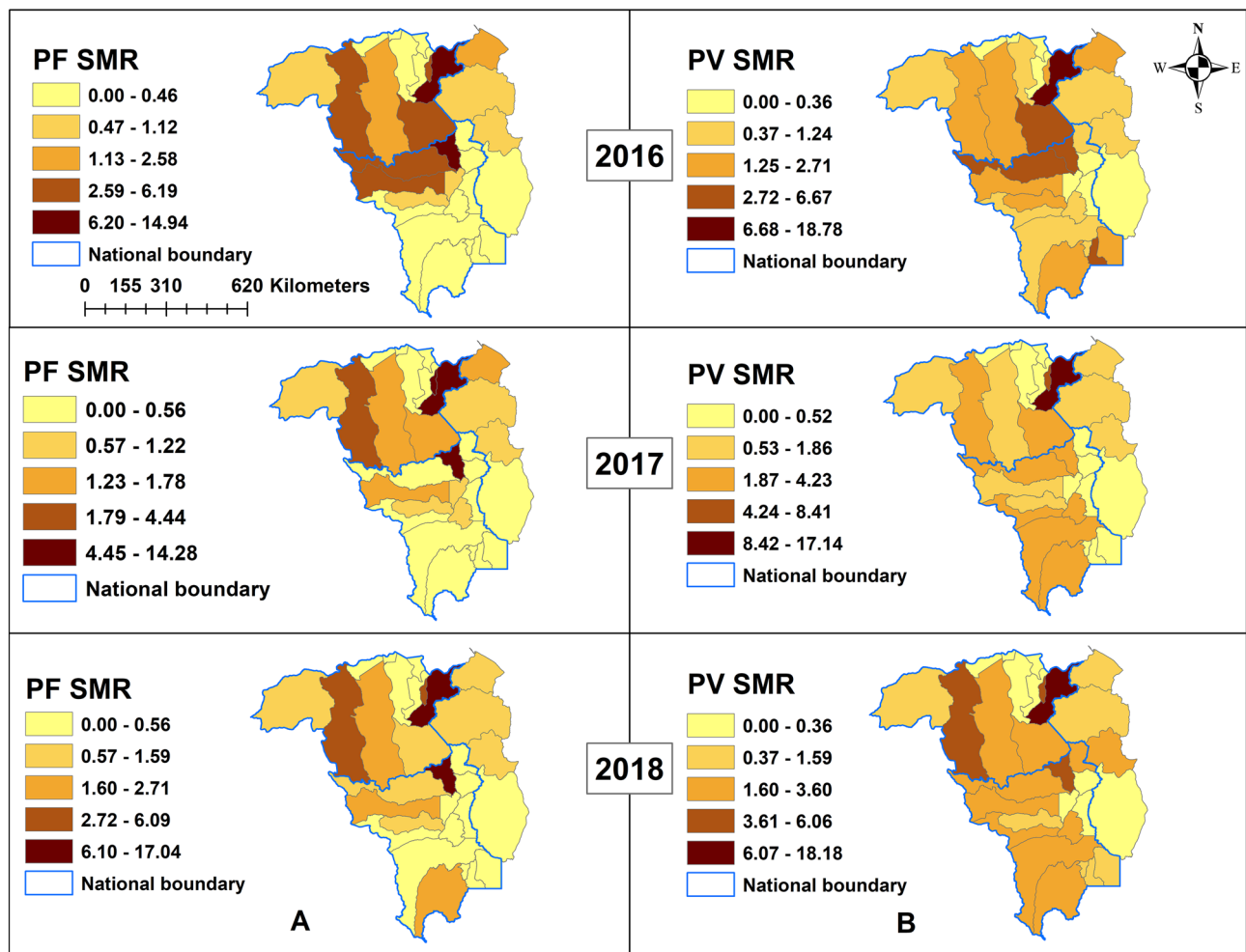


Figure 2. Raw standardized morbidity ratios of (A) *Plasmodium falciparum*. (B) *Plasmodium vivax*, 2016–2018. PF, *Plasmodium falciparum*; PV, *Plasmodium vivax*; SMR, standardized morbidity ratios.

political and economic crisis in Venezuela has thwarted malaria control efforts. Malaria cases have increased significantly in recent years: from 35,500 cases in 2000 to over 467,000 cases in 2019².

Our study showed that malaria hotspots were consistently found in municipalities along the Venezuela-Guyana border with Brazil, including Sifontes municipality, and in municipalities adjacent to Sifontes municipality, including Piar, Padre Pedro Chien, Roscio, and El Callao in Bolivar state. Sifontes municipality was recently identified as the most important cluster of malaria transmission in the Americas⁷. This highlights the issue of cross-border malaria, which can impact malaria control efforts^{35,36}. A plausible solution can be cross-country collaboration to improve surveillance and finding ways to provide early diagnosis and treatment for border populations, which are usually more mobile and difficult to track. Higher cases in these regions have also been related to occupation, especially gold mining³⁷. Gold mining drives increased population movement to mining sites, usually young males⁸. Our findings confirmed this. Males made up two-thirds of cases and more than half of malaria cases were in the 19–40 year age group (Table 1). Furthermore, poor living conditions and working outdoors during late at night or early in the morning also could expose miners to increased mosquito bites.

Plasmodium vivax was the predominant species in this study and is also the primary species in the Americas^{34,38}. Relapse of *P. vivax* is associated with the release of dormant hypnozoites from the liver. Challenges to correct diagnosis include lack of sensitive diagnostic tools. Rapid Diagnostic Tests (RDTs), which are widely used in the region and globally, are unable to diagnose dormant hypnozoites in the liver or in pregnant women. Secondly, adherence to *P. vivax* treatment is a main challenge, which includes a three-day course of chloroquine and 7 or 14 days of primaquine^{39,40}. Hence, continued *P. vivax* transmission in other parts of world has been attributed to lack of adherence to treatment^{41,42}. Since cross-border populations are hard to follow up, we propose implementation of community-based adherence support, which has been used for HIV and TB and has significantly improved treatment^{43–45}. Treatment follow up can be done through a friend or family member who is travelling with the patient or someone who is part of the patient's community such as a community member, a support group, and/or a religious leader.

Altitude was positively associated with both both species of malaria. This is partly explained by the fact that the study area is generally low-lying with altitude ranging from 64.2 to 995.5 meters. Malaria incidence decreased

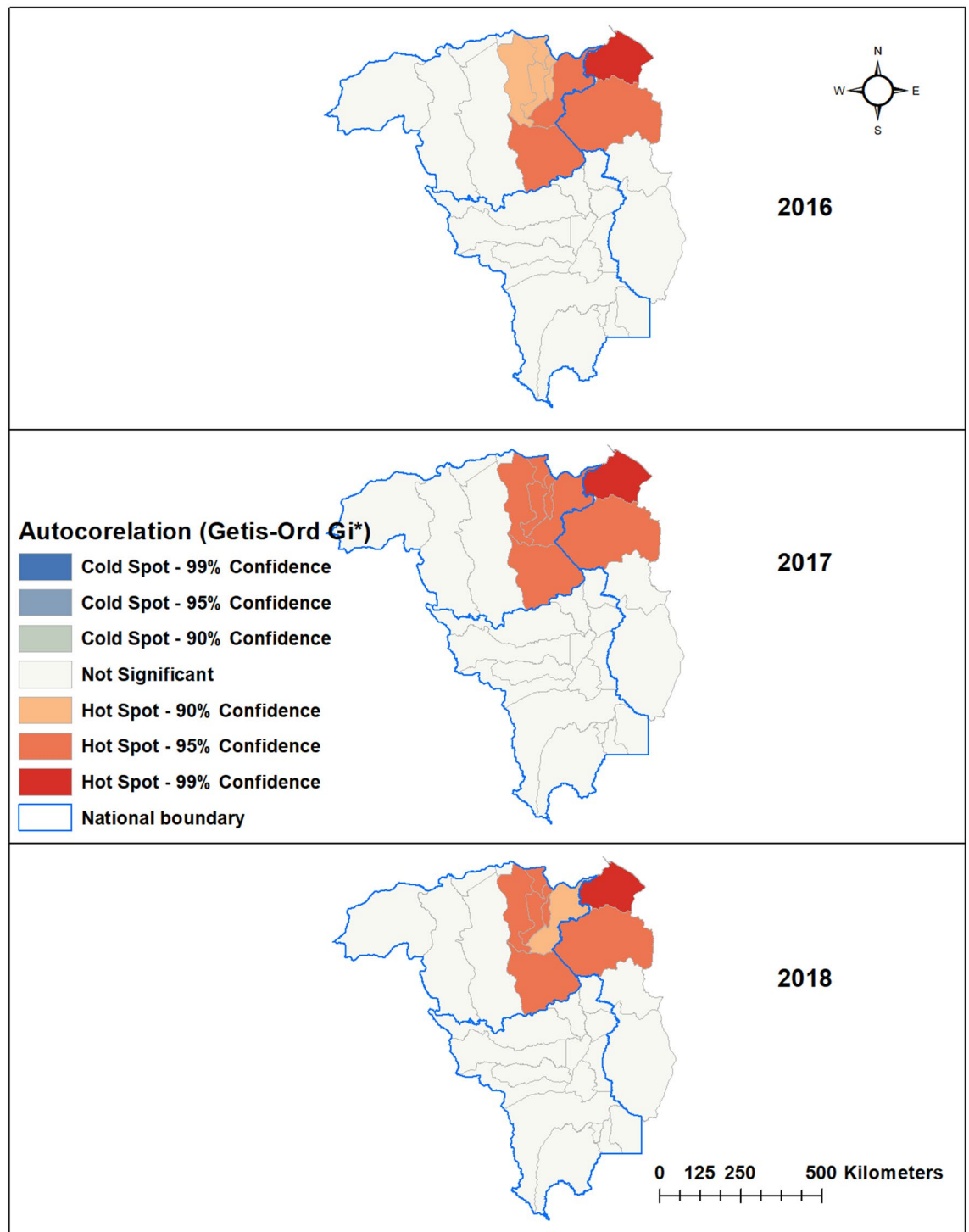


Figure 3. Hot spots (Getis-Ord G_i^*) of *Plasmodium falciparum*.

with increased altitude due to decreases in temperature, which makes the environment unsuitable for *Anopheles* vectors^{46–48}. Further, temperature variation influences the incidence and transmission of infection due to its direct effect on development and survivorship of vectors and malaria parasites⁴⁹.

Climatic variables of precipitation and temperature are also associated with the transmission of malaria in this study. The transmission of the malaria parasite and mosquito survival are affected by temperature^{50,51}. At temperatures of 22 °C, it takes less than three weeks to complete the life cycle of malaria parasite development in the mosquito vector⁵². The biting rate and gonotrophic processes are also temperature dependent^{53,54}. Other studies have reported rainfall as an important driver of malaria transmission^{55,56}. The main vectors responsible for malaria transmission in the Americas, including *Anopheles darlingi* and *An. Albimanus*, are also affected by climate^{57–60}.

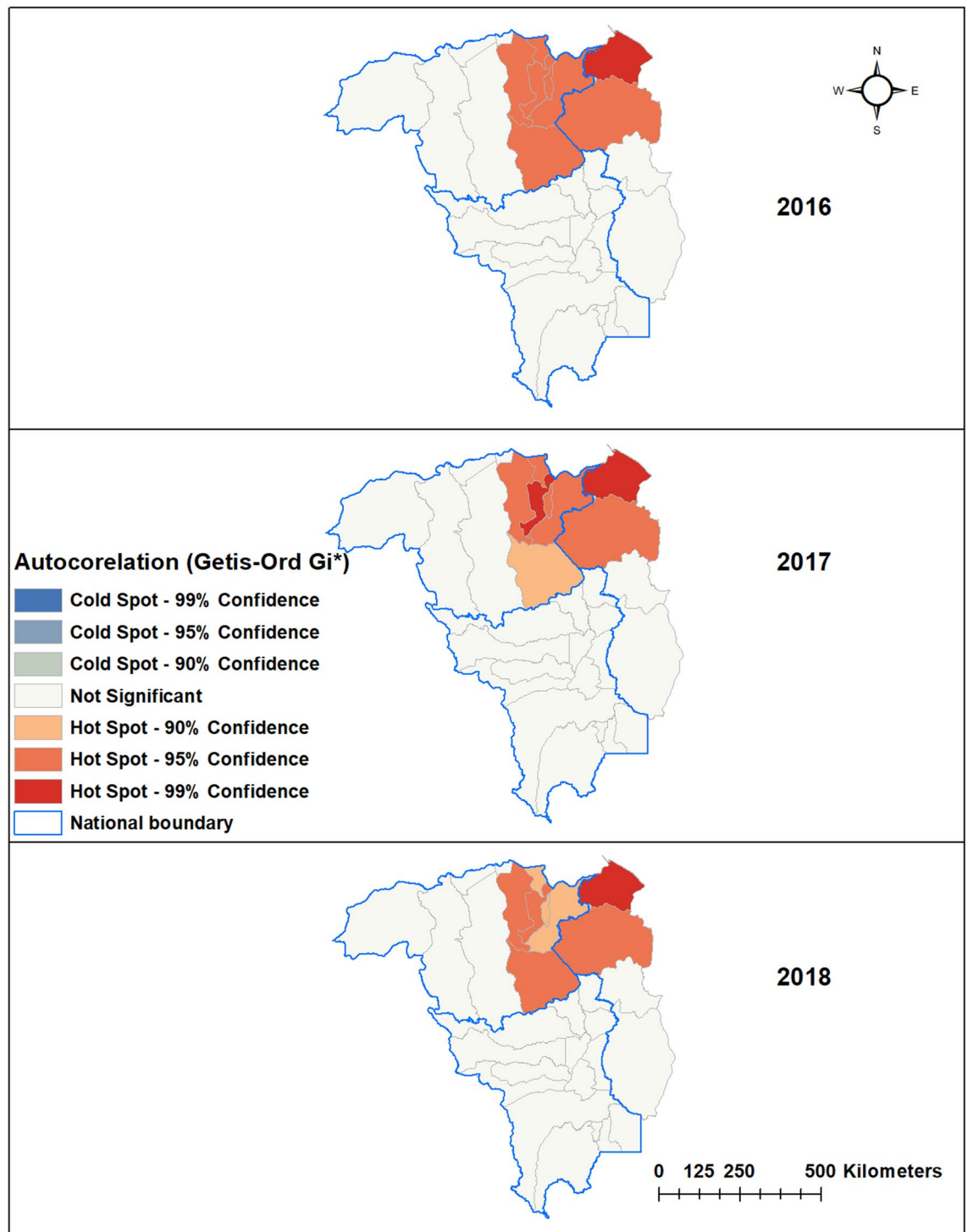


Figure 4. Hot spots (Getis-Ord G_i^*) of *Plasmodium vivax*.

There are some limitations to this study. First, the main limitation is the lack of completeness and representativeness of surveillance data. Second, the true number of malaria cases could have been underestimated if cases were diagnosed and treated in private health settings or self-diagnosed and not captured by the national surveillance system. Third, populations of municipalities were projected, which may have resulted in over or under estimation. Fourth, unmeasured risk modifiers including socio-economic development, living standards, occupation, treatment, localized behavioral patterns, population mobility, and bed net use and residual indoor insecticide coverage were unaccounted for in this study. Fifth, since entomological data were not available, they were not included in the model. Entomological data would have improved the model. Hence, we suggest including these data in further analysis if available.

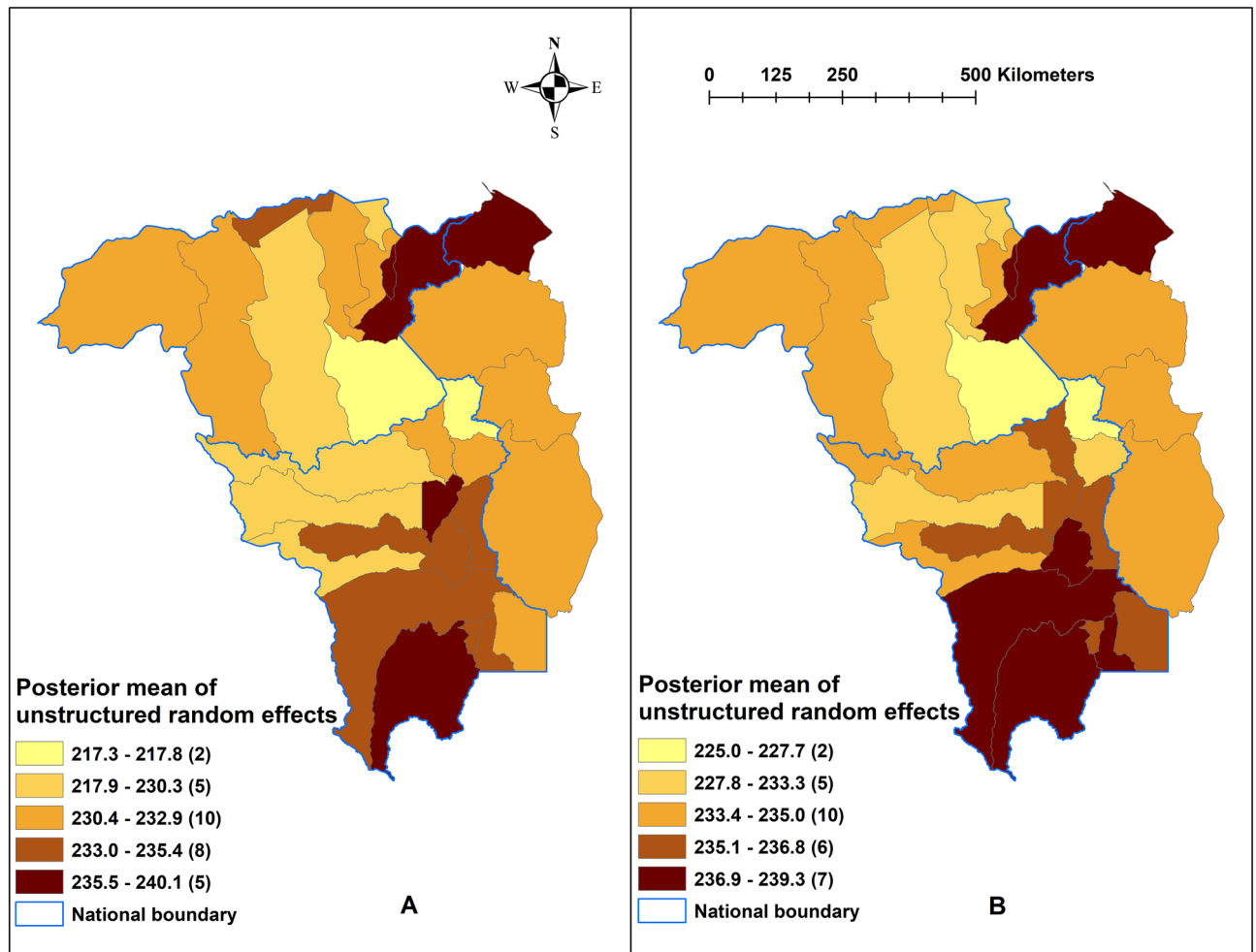


Figure 5. Spatial distribution of the posterior means of unstructured random effects for (A) *Plasmodium falciparum* and (B) *Plasmodium vivax* in Model I.

Conclusion

Plasmodium falciparum and *P. vivax* transmission was negatively associated with increased precipitation and minimum temperature, and positively associated with altitude and maximum temperature. Hotspots of both *P. falciparum* and *P. vivax* were isolated in eight municipalities along the Venezuela and Guyana international border with Brazil. Targeted distribution of resources, including prompt diagnosis and treatment and intensified interventions in hotspot municipalities, will be required for effective control of local malaria transmission. Furthermore, cross-border surveillance needs to be strengthened and ongoing identification of hotspots is needed to stay on track with malaria elimination targets.

Model/variables	<i>Plasmodium falciparum</i> RR (95% CrI)	<i>Plasmodium vivax</i> RR (95% CrI)
Model I		
Monthly trend	1.021 (1.019, 1.021)	1.010 (1.009, 1.010)
Altitude (m)	1.026 (1.021, 1.028)	1.015 (1.013, 1.016)
Precipitation (10 mm)*	0.984 (0.977, 0.985)	0.989 (0.988, 0.990)
Temp min (°C)*	0.991 (0.976, 0.993)	0.927 (0.903, 0.933)
Temp max (°C)**	1.006 (1.004, 1.019)	1.015 (1.006, 1.071)
Heterogeneity		
Unstructured	1.91×10^{-5} (1.08×10^{-5} , 2.98×10^{-5})	1.88×10^{-5} (1.06×10^{-5} , 2.91×10^{-5})
DIC [‡]	50,219	124,173
Model II		
Monthly trend	1.021 (1.020, 1.021)	1.010 (1.009, 1.010)
Altitude (m)	1.013 (1.003, 1.021)	1.009 (1.004, 1.014)
Precipitation (10 mm)*	0.984 (0.977, 0.985)	0.989 (0.988, 0.990)
Temp min (°C)**	0.908 (0.776, 0.927)	0.928 (0.901, 0.934)
Temp max (°C)**	1.063 (1.045, 1.216)	1.014 (1.007, 1.077)
Heterogeneity		
Structured (spatial)	3.77×10^{-2} (1.08×10^{-2} , 1.03×10^{-1})	6.17×10^{-2} (2.10×10^{-2} , 1.43×10^{-1})
DIC	50,888.2	124,413
Model III		
Monthly trend	1.021 (1.020, 1.021)	1.016 (1.009, 1.010)
Altitude (m)	1.030 (1.028, 1.032)	1.018 (1.014, 1.021)
Precipitation (10 mm)*	0.984 (0.978, 0.985)	0.989 (0.988, 0.990)
Temp min (°C)**	0.906 (0.774, 0.927)	0.928 (0.905, 0.934)
Temp max (°C)**	1.063 (1.047, 1.217)	1.015 (1.007, 1.074)
Heterogeneity		
Unstructured	2.66×10^{-4} (1.49×10^{-4} , 4.19×10^{-4})	3.51×10^{-4} (1.99×10^{-4} , 5.47×10^{-4})
Structured (spatial)	9.77×10^{-4} (5.28×10^{-5} , 1.57×10^{-4})	1.25×10^{-4} (6.93×10^{-5} , 1.98×10^{-4})
DIC	51,059.5	124,422

Table 2. Regression coefficients, relative risks and 95% CrI from Bayesian spatial and non-spatial models for *Plasmodium falciparum* and *Plasmodium vivax* from 2016 to 2018. CrI, credible interval; DIC, deviation information criteria; RR, relative risk. [‡]Best fit model. *Precipitation lagged at 6-months for both *Plasmodium falciparum* and *P. vivax*. **No lag and 6-months lag for *P. falciparum* and *P. vivax*. ***1 and 2-months lagged for *P. falciparum* and *P. vivax*.

Data availability

The study dataset can be made available only upon the approval by researchers and organizations involved.

Received: 6 January 2022; Accepted: 31 May 2022

Published online: 29 June 2022

References

1. WHO. World Malaria Report 2021 (World Health Organization, 2021).
2. WHO. World Malaria Report 2020 (World Health Organization, 2020).
3. Burton, R. A. *et al.* Factors associated with the rapid and durable decline in malaria incidence in El Salvador, 1980–2017. *Am. J. Trop. Med. Hyg.* **99**, 33–42 (2018).
4. Grillet, M. E. *et al.* Venezuela's humanitarian crisis, resurgence of vector-borne diseases, and implications for spillover in the region. *Lancet Infect. Dis.* **19**, e149–e161 (2019).
5. Rodríguez-Morales, A. J. & Paniz-Mondolfi, A. E. Venezuela's failure in malaria control. *Lancet* **384**, 663–664 (2014).
6. Oletta, J. F., Orihuela, R. A., Pulido, P. & Walter, C. Venezuela: violence, human rights, and health-care realities. *Lancet* **383**, 1967 (2014).
7. Grillet, M. E. *et al.* Malaria in Southern Venezuela: the hottest hotspot in Latin America. *PLoS Negl. Trop. Dis.* **15**, e0008211 (2021).
8. Recht, J. *et al.* Malaria in Brazil, Colombia, Peru and Venezuela: current challenges in malaria control and elimination. *Malar. J.* **16**, 273 (2017).
9. Recht, J. *et al.* *Malaria Transmission in South America- Present Status and Prospects for Elimination* (IntechOpen, 2018).
10. Wangdi, K. *et al.* A spatio-temporal analysis to identify the drivers of malaria transmission in Bhutan. *Sci. Rep.* **10**, 7060 (2020).
11. Clements, A. C. A., Reid, H. L., Kelly, G. C. & Hay, S. I. Further shrinking the malaria map: how can geospatial science help to achieve malaria elimination?. *Lancet Infect. Dis.* **13**, 709–718 (2013).
12. Wangdi, K. *et al.* Malaria elimination in India and regional implications. *Lancet Infect. Dis.* **16**, e214–e224 (2016).
13. Wangdi, K. *et al.* Development of temporal modelling for forecasting and prediction of malaria infections using time-series and ARIMAX analyses: a case study in endemic districts of Bhutan. *Malar. J.* **9**, 251 (2010).

14. Sweeney AW. The Application of GIS in Malaria Control Programs. 10th Colloquium of the Spatial Information Research Centre, University of Otago, New Zealand, 16–19 November (1998).
15. Richards, T. B., Croner, C. M., Rushton, G., Brown, C. K. & Fowler, L. Geographic information systems and public health: mapping the future. *Public Health Rep.* **114**, 359–373 (1999).
16. Malone, J. B., Bergquist, R., Martins, M. & Luvall, J. C. Use of geospatial surveillance and response systems for vector-borne diseases in the elimination phase. *Trop. Med. Infect. Dis.* **4**, 15 (2019).
17. Wangdi, K. *et al.* Development and evaluation of a spatial decision support system for malaria elimination in Bhutan. *Malar. J.* **15**, 180 (2016).
18. Wangdi, K. *et al.* Spatial and temporal patterns of malaria in Phu Yen Province, Vietnam, from 2005 to 2016. *Am. J. Trop. Med. Hyg.* **103**, 1540–1548 (2020).
19. Wangdi, K. & Clements, A. C. Spatial and temporal patterns of diarrhoea in Bhutan 2003–2013. *BMC Infect. Dis.* **17**, 507 (2017).
20. Wangdi, K., Clements, A. C. A., Du, T. & Nery, S. V. Spatial and temporal patterns of dengue infections in Timor-Leste, 2005–2013. *Parasit Vectors* **11**, 9 (2018).
21. Kelly, G. C. *et al.* A high-resolution geospatial surveillance-response system for malaria elimination in Solomon Islands and Vanuatu. *Malar. J.* **12**, 108 (2013).
22. Kelly, G. C. *et al.* A spatial decision support system for guiding focal indoor residual spraying interventions in a malaria elimination zone. *Geospat. Health* **6**, 21–31 (2011).
23. Kelly, G. C., Tanner, M., Vallely, A. & Clements, A. Malaria elimination: moving forward with spatial decision support systems. *Trends Parasitol* **28**, 297–304 (2012).
24. Kalluri, S., Gilruth, P., Rogers, D. & Szczur, M. Surveillance of arthropod vector-borne infectious diseases using remote sensing techniques: a review. *PLoS Pathog.* **3**, 1361–1371 (2007).
25. IBGE Censo 2010. <https://censo2010.ibge.gov.br/sinopse/>.
26. INE. Venezuela Census 2011 (2018).
27. Historical climate data. <https://www.worldclim.org/data/worldclim21.html>.
28. Anselin, L. & Getis, A. Spatial statistical analysis and geographic information systems. *Ann. Reg. Sci.* **26**, 19–33 (1992).
29. Ord, J. K. & Getis, A. Local spatial autocorrelation statistics: distributional issues and an application. *Geogr. Anal.* **27**, 286–306 (1995).
30. Zulu, L. C., Kalipeni, E. & Johannes, E. Analyzing spatial clustering and the spatiotemporal nature and trends of HIV/AIDS prevalence using GIS: the case of Malawi, 1994–2010. *BMC Infect. Dis.* **14**, 285 (2014).
31. Moreno, J. E., Rubio-Palis, Y., Martínez, Á. R. & Acevedo, P. Evolución espacial y temporal de la malaria en el municipio Sifontes del estado Bolívar, Venezuela. 1980–2013. *J. Bol. Malariol. Salud Ambient.* **54**, 236–249 (2014).
32. Grillet, M. E., El Souki, M., Laguna, F. & León, J. R. The periodicity of *Plasmodium vivax* and *Plasmodium falciparum* in Venezuela. *Acta Trop.* **129**, 52–60 (2014).
33. Gabaldón-Figueira, J. C., Chaccour, C., Moreno, J., Villegas, M. & Villegas, L. The malaria burden of Amerindian groups of three Venezuelan states: a descriptive study based on programmatic data. *Malar. J.* **20**, 285 (2021).
34. Douine, M. *et al.* Malaria in gold miners in the guianas and the amazon: current knowledge and challenges. *Curr. Trop. Med. Rep.* **7**, 37–47 (2020).
35. Wangdi, K., Gatton, M. L., Kelly, G. C. & Clements, A. C. Cross-border malaria: a major obstacle for malaria elimination. *Adv. Parasitol.* **89**, 79–107 (2015).
36. Wangdi, K., Pasaribu, A. P. & Clements, A. C. A. Addressing hard-to-reach populations for achieving malaria elimination in the Asia Pacific Malaria Elimination Network countries. *Asia Pac. Policy Stud.* **8**, 176–188 (2021).
37. Arisco, N. J., Peterka, C. & Castro, M. C. Cross-border malaria in Northern Brazil. *Malar. J.* **20**, 135 (2021).
38. de Oliveira, E. C., dos Santos, E. S., Zeilhofer, P., Souza-Santos, R. & Atanaka-Santos, M. Geographic information systems and logistic regression for high-resolution malaria risk mapping in a rural settlement of the southern Brazilian Amazon. *Malar. J.* **12**, 420 (2013).
39. Wangchuk, S. *et al.* Where chloroquine still works: the genetic make-up and susceptibility of *Plasmodium vivax* to chloroquine plus primaquine in Bhutan. *Malar. J.* **15**, 277 (2016).
40. Thriemer, K. *et al.* Quantifying primaquine effectiveness and improving adherence: a round table discussion of the APMEN Vivax Working Group. *Malar. J.* **17**, 241 (2018).
41. Grietens, K. P. *et al.* Adherence to 7-day primaquine treatment for the radical cure of *P. vivax* in the Peruvian Amazon. *Am. J. Trop. Med. Hyg.* **82**, 1017–1023 (2010).
42. Pereira, E. A., Ishikawa, E. A. & Fontes, C. J. Adherence to *Plasmodium vivax* malaria treatment in the Brazilian Amazon Region. *Malar. J.* **10**, 355 (2011).
43. Rogers, J. H. *et al.* Impact of community-based adherence support on treatment outcomes for tuberculosis, leprosy and HIV/AIDS-infected individuals in post-Ebola Liberia. *Glob. Health Action* **11**, 1522150 (2018).
44. Grimwood, A. *et al.* Community adherence support improves programme retention in children on antiretroviral treatment: a multicentre cohort study in South Africa. *J. Int. AIDS Soc.* **15**, 17381 (2012).
45. Community Adherence Clubs. Breaking down barriers to treatment in Namibia. <https://www.cdc.gov/globalhivtb/who-we-are/success-stories/success-story-pages/communityadherenceclubs.html>.
46. Dabaro, D., Birhanu, Z., Negash, A., Hawaria, D. & Yewhalaw, D. Effects of rainfall, temperature and topography on malaria incidence in elimination targeted district of Ethiopia. *Malar. J.* **20**, 104 (2021).
47. Dhiman, R. C., Yadav, Y. K., Saraswat, S. & Singh, P. Altitude, temperature, and malaria vectors in Nainital and Udham Singh Nagar districts of Uttarakhand, India: an evidence-based study. *J. Vector Borne Dis.* **50**, 220–224 (2013).
48. Guerra, C. A., Snow, R. W. & Hay, S. I. Defining the global spatial limits of malaria transmission in 2005. *Adv. Parasitol.* **62**, 157–179 (2006).
49. Fouque, F. & Reeder, J. C. Impact of past and on-going changes on climate and weather on vector-borne diseases transmission: a look at the evidence. *Infect. Dis. Poverty* **8**, 51 (2019).
50. Brooker, S. *et al.* Spatial clustering of malaria and associated risk factors during an epidemic in a highland area of western Kenya. *Trop. Med. Int. Health* **9**, 757–766 (2004).
51. Noden, B. H., Kent, M. D. & Beier, J. C. The impact of variations in temperature on early *Plasmodium falciparum* development in *Anopheles stephensi*. *Parasitology* **111**(Pt 5), 539–545 (1995).
52. Teklehaimanot, H. D., Lipsitch, M., Teklehaimanot, A. & Schwartz, J. Weather-based prediction of *Plasmodium falciparum* malaria in epidemic-prone regions of Ethiopia I. Patterns of lagged weather effects reflect biological mechanisms. *Malar. J.* **3**, 41 (2004).
53. Tompkins, A. M. & Erment, V. A regional-scale, high resolution dynamical malaria model that accounts for population density, climate and surface hydrology. *Malar. J.* **12**, 65 (2013).
54. Paaijmans, K. P. *et al.* Influence of climate on malaria transmission depends on daily temperature variation. *Proc. Natl. Acad. Sci. U. S. A.* **107**, 15135–15139 (2010).
55. Craig, M. H., Snow, R. W. & le Sueur, D. A climate-based distribution model of malaria transmission in sub-Saharan Africa. *Parasitol. Today* **15**, 105–111 (1999).
56. Thomson, M. C., Mason, S. J., Phindela, T. & Connor, S. J. Use of rainfall and sea surface temperature monitoring for malaria early warning in Botswana. *Am. J. Trop. Med. Hyg.* **73**, 214–221 (2005).

57. Zimmerman, R. H. Ecology of malaria vectors in the Americas and future direction. *Mem. Inst. Oswaldo Cruz.* **87**(Suppl 3), 371–383 (1992).
58. Laporta, G. Z. *et al.* Malaria vectors in South America: current and future scenarios. *Parasit. Vectors.* **8**, 426 (2015).
59. Batista, E. P., Costa, E. F. & Silva, A. A. *Anopheles darlingi* (Diptera: Culicidae) displays increased attractiveness to infected individuals with *Plasmodium vivax* gametocytes. *Parasit. Vectors* **7**, 251 (2014).
60. Rios-Velázquez, C. M. *et al.* Experimental *Plasmodium vivax* infection of key *Anopheles* species from the Brazilian Amazon. *Malar. J.* **12**, 460 (2013).

Acknowledgements

Authors would like to thank the Ministries of Health of Brazil, Guyana and Venezuela for sharing the data, and all of the health workers in Roraima, Bolívar, and Guyana for their contributions to collecting and reporting the data. We would also like to thank Jorge Moreno (Centro de Investigación de Campo Francisco Vitanza, Tumeremo, Bolívar, Venezuela) and Maria Villegas (Global Development One, Silver Spring, Maryland, USA) who supported data acquisition and entry for the data from Bolívar state.

Author contributions

All authors were involved in the conceptualization and design of the study. E.W., H.C., P.M., L.V. and S.C. were involved in data acquisition. K.W. and E.W. undertook the data cleaning and statistical analysis. K.W. drafted the manuscript. E.W., H.C., P.M., L.V. and S.C. provided critical revision of the manuscript. All authors read and approved the final manuscript.

Funding

This study was supported by World Vision US, Global Development One, USA, and Asociacion Civil Impacto Social (ASOCIS), Venezuela.

Competing interests

The authors declare no competing interests.

Additional information

Supplementary Information The online version contains supplementary material available at <https://doi.org/10.1038/s41598-022-14012-4>.

Correspondence and requests for materials should be addressed to K.W.

Reprints and permissions information is available at www.nature.com/reprints.

Publisher's note Springer Nature remains neutral with regard to jurisdictional claims in published maps and institutional affiliations.



Open Access This article is licensed under a Creative Commons Attribution 4.0 International License, which permits use, sharing, adaptation, distribution and reproduction in any medium or format, as long as you give appropriate credit to the original author(s) and the source, provide a link to the Creative Commons licence, and indicate if changes were made. The images or other third party material in this article are included in the article's Creative Commons licence, unless indicated otherwise in a credit line to the material. If material is not included in the article's Creative Commons licence and your intended use is not permitted by statutory regulation or exceeds the permitted use, you will need to obtain permission directly from the copyright holder. To view a copy of this licence, visit <http://creativecommons.org/licenses/by/4.0/>.

© The Author(s) 2022